Received: 04 July 2023, Accepted: 15 August 2023

Original Research

Journal of Advanced Veterinary Research
(2023) Volume 13, Issue 8, 1575-1582

Oral Administration of Thymoquinone Attenuates Diazinon-induced Renal Injury in Rat: The Involvement of Keap1/Nrf2/HO1/NQO Signaling Pathway

Eman M. Fath[1], Hatem H. Bakery[1], Ragab M. EL-Shawarby[1], Mohamed E.S. Abosalem[1], Nesrine Ebrahim[2,3,4], Ahmed Medhat Hegazy[1*], Samer S. Ibrahim[1]

[1]Department of Forensic Medicine and Toxicology, Faculty of Veterinary Medicine, Benha University, Moshtohor, Toukh 13736, Qalyubia, Egypt.

[2]Department of Histology and Cell Biology Faculty of Medicine, Benha University, Benha 13511, Egypt.

[3]Stem Cell Unit, Faculty of Medicine, Benha University, Benha 13511, Egypt.

[4]Benha National University, Faculty of Medicine, Obour City, Egypt.

***Correspondence**
Corresponding author: Ahmed Medhat Hegazy
E-mail address: ahmed.hegazy@fvtm.bu.edu.eg

Abstract

The most prevalent component of the volatile oil found in *Nigella sativa* seeds is thymoquinone (TQ). As well as being used as food supplements, the seeds and oil are also utilized in traditional medicine to treat a variety of ailments. The purpose of this investigation was to determine whether TQ could protect rats from acute nephrotoxicity caused by diazinon (DZN). Six equal groups of thirty six adult male Wistar rats were created at random. Group 1 (G1) was maintained in typical control circumstances and given saline daily intragastric (IG) for 4 weeks; G2 was administered 0.1 mL olive oil IG for 4 weeks; G3 was administered 0.1 mL DMSO IG for 4 weeks; G4 was administered IG TQ at a dose of 10 mg/kg B.W. daily for 4 weeks; G5 was administered IG DZN at a dose of 15 mg/kg B.W. daily for 4 weeks; G6 was administered TQ intragastric (IG) daily, one hour before DZN at the same dose as in G4 and G5, for 4 weeks. The findings showed that TQ reduces the renal dysfunctions brought on by DZN by restoring urea and creatinine levels as well as oxidative indicators. Although the expression of Kelch-like ECH-associated protein 1 (Keap1) was also elevated, overexpression of nuclear factor erythroid 2–related factor 2 (Nrf2) also enhanced the expression of heme oxygenase-1 (HO-1), and Nuclear factor kappa B (NFκB) in renal tissue. Also, TQ increased antiapoptotic (BCL2) factors and decrease proapoptotic (BAX) factors. In conclusion, TQ is helpful in the prevention and management of acute nephrotoxicity brought on by DZN.

KEYWORDS
Diazinon, Heme oxygenase-1, Nephrotoxicity, Oxidative stress, Thymoquinone.

INTRODUCTION

A class of insecticides known as organophosphorus pesticides (OPs) are made from phosphoric or phosphorothioate acid (Boussabbeh *et al*., 2016). Over the next ten years, there is a predicted increase in the danger of pesticide exposure worldwide, especially in emerging nations (Wang *et al*., 2022). Acute exposure to OPs results in over three million life-threatening poisonings annually, over 250,000 self-poisoning fatalities, and nearly one-third of all suicide cases worldwide (Guignet *et al*., 2020). In recent years, agricultural use of the organophosphate insecticide diazinon (DZN) has increased significantly. DZN can cause biochemical, physiological, and histological changes in a variety of organs, including the liver, kidney, heart, testis, and brain (Jiang *et al*., 2022).

The NLRP3 (Nod-like receptor pyrin domain containing 3) inflammasome is one of the multi-protein complexes known as inflammasomes connected to the innate immune system of pyroptosis (El-Shaer *et al*., 2023). The caspase-1-dependent synthesis of IL-1β (interleukin-1β) is accelerated by the ROS (reactive oxygen species), which activates NLRP3 (Yu *et al*., 2020). Oxidative stress, pro-inflammatory activity, and DNA disruption were the results of these effects (Danaei *et al*., 2019).

One such miraculous herb, *Nigella sativa* (NS), has been utilized for ages in Asia, the Middle East, and Africa as a folk remedy (Jakhmola Mani *et al*., 2022). Traditional uses of the NS seeds, oil, and some of its medicinal ingredients, including thymoquinone (TQ), include the treatment of renal, liver, stomach, pulmonary, and intestinal ailments (Prairna *et al*., 2022). *Nigella sativa* volatile oil contains TQ in the highest concentration (Kizi and Kizi, 2022). It has anti-inflammatory and antioxidant properties that may be used to effectively mitigate the negative impacts of environmental contaminants (Salem *et al*., 2023). The objective of the current studies was to evaluate the potential protective and immunomodulatory effects of thymoquinone on the kidney functions of Wistar rats exposed to DZN induced renal damage.

MATERIALS AND METHODS

Ethical approval

Regulations set forth by the Institutional Animal Ethics Committee were followed when conducting the current investigation, as well as Approval Protocol Number: BUFVTM 03-04-21 from Benha University in Egypt.

Chemicals

Thymoquinone (TQ), olive oil, and dimethyl sulphoxide (DMSO) were purchased from Aldrich Company, USA. Diazinon

ISSN: 2090-6277/2090-6269/

(DZN) was purchased from High Control Company in Naser City, Cairo, Egypt.

Experimental animals

Six weeks old male adult Wistar rats (weighing 125 to 145 g) were purchased from the Faculty of Veterinary Medicine, Experimental Animal Unit, Benha University, Egypt. Rats were housed in orderly cages and were provided with clean food and water on demand. All rats were kept in standard conditions, including a room temperature of 23°C, a 12-hour light/dark cycle, and free water and food were available. Prior to therapy, baseline body weight measurements were performed for all groups. Weekly animal weights were taken in order to modify the chemical dosage.

Experimental design

Six equal groups of six adult male Wistar rats each were created from a total of 36 rats. The initial group (G1) was kept as a healthy control and given 0.1 mL intragastric saline once daily for 4 weeks. The second group (G2) was administered 0.1 mL olive oil once daily for 4 weeks. The third group (G3) was administered 0.1 mL DMSO intragastric daily for 4 weeks. The fourth group (G4) was administered intragastric TQ (dissolved in DMSO) at a dose of 10 mg/kg b.wt. daily for 4 weeks (Danaei and Karami, 2017). The fifth group (G5) was administered DZN (dissolved in olive oil) intragastric at a dose of 15 mg/kg B.W. daily for 4 weeks (Rashedinia *et al*., 2016). The six group (G6) was administered intragastric TQ daily one hour before DZN at the same dose in G4 and G5 daily for 4 weeks. The experimental rats were euthanized with isoflurane after the study was completed before being killed by decapitation, then blood samples were collected from the heart for estimation of blood urea, and creatinine levels. The kidney specimens were quickly removed and weighed, then washed with cold saline to exclude the blood cells and then blotted on filter paper; the kidney was divided into three parts. The first part was suspended in 4 ml physiological saline (0.9 % NaCl) for homogenization. The tissue homogenates were centrifuged 1500xg for 20 minutes at 4ºC. The supernatants were kept at -20ºC till the time of determination of oxidative/antioxidant parameters. The second part was kept in RNAlater storage reagent for gene expression at -80ºC. The third part was placed in 10 % formalin solution for histopathological investigations. The kidney specimens were collected for estimation of oxidative markers included catalase (CAT), superoxide dismutase (SOD), glutathione peroxidase (GPx), reduced glutathione (GSH), malondialdehyde (MDA); gene expression includes NLRP3, Nrf2, Keap-1, NQO; and the histopathological changes in kidney.

Preparation of kidney homogenate

Kidney tissue homogenate was performed according to Hegazy *et al*. (2020). The collected supernatant was used for determination of the oxidant/antioxidant markers [lipid peroxidation by-products malondialdehyde (MDA) level, catalase (CAT), superoxide dismutase (SOD) activity, glutathione peroxidase (GPx), and reduced glutathione (GSH) concentration], kidney proteins [Nrf2, Kelch-like ECH-associated protein 1 (Keap1), heme oxygenase-1 (HO-1), Nuclear factor kappa B (NFκB) and β-actin], and the total protein.

Assay methods

Kidney function tests

Serum urea and creatinine concentrations were performed by Bio-Diagnostic commercially available kits according to Skeggs (1957) and Weissman *et al*. (1974); respectively.

Oxidative markers in kidney tissue homogenate

According to using commercially available ELISA kits (Biovision Inc. 155S Milpitas Blvd, Milpitas, CA, 95035 USA); catalase (CAT), superoxide dismutase (SOD), glutathione peroxidase (GSH-Px), reduced glutathione (GSH) and malondialdehyde (MDA) were determined. Based on Bradford (1976) method, the tissue homogenate's protein content was measured using Genei, Bangalore, protein estimation kit. An Enzyme-Linked Immuno-Sorbent Assay (ELISA) plate reader (Stat Fax 2200, Awareness Technologies, Florida, USA) was used to measure color absorbance.

Apoptotic markers in kidney tissue homogenate

BCL2, BAX and IL-1β were determined using commercially available ELISA kits (Cloud-Clone Corp Co., Houston, USA) in line with the instructions provided by the manufacturer.

Kidney mRNA gene expression

Real-time polymerase chain reaction (PCR) was used to assess the mRNA gene expression of the kidney's NLRP3, nuclear factor erythroid 2–related factor 2 (Nrf2), Keap1, and NQO genes. The following primer sets were utilized: NLRP3, Nrf2, Keap1, NQO and GAPDH (Table 1). Thermal cycling and fluorescence detection were carried out using an Applied Biosystems 7300 real-time PCR system (Foster City, California, USA). Cycle threshold (Ct) values acquired from real-time PCR equipment were applied to a reference (housekeeping) gene (GAPDH) to detect changes in gene expression (Livak and Schmittgen, 2001).

Protein markers in kidney tissue homogenate

We used the Bio-Rad Inc. ReadyPrepTM protein extraction kit (Catalogue #163-2086) for kidney tissue proteins extraction. Protein concentrations were measured using the Bradford Protein Assay Kit (SK3041) from Bio Basic INC (Markham, Ontario,

Table 1. Primer's sequence of all studied genes.

Gene symbol	Forward	Reverse	Gene bank
NLRP3	GTAGGTGTGGAAGCAGGACT	CTTGCTGACTGAGGACCTGA	XR_005489722.1
Nrf2	GCAACTCCAGAAGGAACAGG	AGGCATCTTGTTTGGGAATG	NM_031789.2
Keap1	GGAATGCTATGACCCAGACA	TGCTCAGGTAGTCCAAGTGC	XM_032909789.1
NQO	AAAGGACCCTTCCGGAGTAA	CGTTTCTTCCATCCTTCCAG	NM_000903.3
GAPDH	CACCCTGTTGCTGTAGCCATATTC	ACATCAAGAAGGTGGTGAAGCAG	XM_032910454.1

L3R 8T4 Canada). The loading quantity of protein samples were 20µg. The extracts were separated by Sodium Dodecyl Sulfate Polyacrylamide Gel Electrophoresis (SDS-PAGE) (12%), and then transferred to polyvinylidene fluoride (PVDF) membrane (7min at 25V). After blocking the membrane for an hour at room temperature with tris-buffered saline with Tween 20 (TBST) buffer and 3% bovine serum albumin (BSA), the membrane was subjected to a variety of primary antibodies. Primary antibodies of NFκB, HO-1, Keap1, Nrf2, and β-actin were purchased from OriGene Technologies Inc (9620 Medical Center Drive, Ste 200 Rockville, MD 20850, USA). Then the primary antibodies were treated at 4oC overnight as anti-NFκB, anti-HO-1, anti-Keap1, anti-Nrf2, and anti-β actin (housekeeping protein). For five minutes, the blot was being rinsed with TBST 3-5 times. The goat anti-rabbit IgG- HRP-1 mg Goat mab- Novus Biologicals secondary antibody solution was treated with the target protein for 1 hour at room temperature. The blot was then rinsed with TBST three times for five minutes. The blot was covered with the chemiluminescent substrate (Catalogue no. 170-5060, ClarityTM Western ECL substrate Bio-Rad). The chemiluminescent signals were captured using an imager that is based on a CCD camera. By protein normalization on the ChemiDoc MP Imager, band intensity of the target proteins was read against the control sample β-actin (housekeeping protein).

Histopathological examination

All groups had kidney samples collected right away, which were then fixed for 24 hours in 10% buffered neutral formalin. Following convenient fixing, the samples were cleaned in xylol, embedded in paraffin, dehydrated in various grades of ethyl alcohol, blocked, and sectioned into 4µm thick sections. Followed by hematoxylin and eosin, and Masson's trichrome staining and microscopic examination (Suvarna *et al*., 2018).

Immunohistochemical study

Deparaffinized and hydrated paraffin sections were used. The sections were first blocked for non-specific reactions with 10% hydrogen peroxide, followed by incubation with primary rabbit polyclonal antibodies against rabbit monoclonal antibodies [E63] to BAX (ab32503), 1/250 dilution; abcam, UK); a concentration of 2-4 µg/ml was used. Before beginning with IHC staining technique (Abcam, UK) and rabbit polyclonal to SERCA2 ATPase (ab3625, a concentration of 1 g/ml was used), do heat-mediated antigen retrieval with citrate buffer pH 6. Before beginning the IHC staining process, perform heat-mediated antigen retrieval (Abcam, UK). Next, a biotinylated goat anti-rabbit secondary antibody was used after phosphate buffer washed the cells. To localize the immunological response, the slides were treated with labelled avidin-biotin peroxidase, which binds to the biotin on the secondary antibody. For visualizing the location where an antibody binds and peroxidase transforms it into a brown precipitate, diaminobenzidine was used as a chromogen (Suvarna *et al*., 2013).

Morphometric study

Using the Image-Pro Plus programme version 6.0 (Media Cybernetics Inc., Bethesda, Maryland, USA), the mean area% of collagen fiber deposition, and BAX immuno-expression were calculated. The mean area% for each marker was determined for five photographs taken from five different fields for each rat in each group.

Statistical analysis

The statistical analysis was completed using the SPSS for Windows (Version 18.0; SPSS Inc., Chicago, Illinois) statistical software for social research. With Duncan's post hoc analysis, the one-way ANOVA test was utilized to identify significant differences between experimental groups. The mean and standard error of the mean (SEM) are used to express results. A P values lower than 0.05 were regarded as significant.

RESULTS

All through the research period, there were no deaths reported among the various treatment groups.

Kidney function tests

Table 2 displays the mean and standard error of serum urea and creatinine levels for the various groups. After 30 days, the DZN treated group (G5) had significantly higher serum urea and creatinine levels than the normal control, olive oil, DMSO, and TQ groups. The serum urea and creatinine levels of intoxicated rats treated with TQ, in contrast to the DZN group, significantly decreased after 30 days of treatment.

Table 2. Effect of thymoquinone (TQ) against diazinone (DZN) on kidney function tests in various gatherings of the experiment after 30 days of treatment, (n=6)

Groups	Control	Olive oil	DMSO	TQ	DZN	TQ+DZN
Urea (mg/dL)	27.04±1.30^{a}	27.64±1.87^{a}	32.05±1.77^{a}	29.05±1.67^{a}	91.98±5.16^{c}	56.16±4.83^{b}
Creatinine (mg/dL)	0.68±0.02^{a}	0.59±0.02^{a}	0.75±0.22^{a}	0.85±0.05^{a}	4.38±0.44^{c}	2.21±0.14^{b}

Data are expressed as mean±standard error. Means with different superscripts in the same row are significantly different at p<0.05.

Table 3. Effect of thymoquinone (TQ) against diazinone (DZN) on oxidative markers in the kidney homogenates of various gatherings of the experiment after 30 days of treatment, (n=6).

Groups	Control	Olive oil	DMSO	TQ	DZN	TQ+DZN
CAT (U/mg protein)	2.37±0.05^{b}	2.58±0.39^{b}	2.70±0.22^{b}	2.72±0.20^{b}	1.25±0.07^{a}	2.30±0.20^{b}
SOD (U/mg protein)	3.00±0.16^{b}	2.97±0.12^{b}	2.90±0.12^{b}	2.86±0.12^{b}	0.95±0.07^{a}	2.70±0.09^{b}
GPx (nmol/mg protein)	25.20±0.74^{b}	24.86±1.82^{b}	23.40±1.80^{b}	23.02±1.17^{b}	10.60±0.50^{a}	21.68±0.78^{b}
GSH (µg/mg protein)	1.69±0.08^{b}	1.70±0.10^{b}	1.47±0.04^{b}	1.58±0.09^{b}	0.45±0.04^{a}	1.48±0.08^{b}
MDA (nmol/mg protein)	0.36±0.03^{a}	0.34±0.01^{a}	0.27±0.00^{a}	0.27±0.00^{a}	2.38±0.19^{b}	0.58±0.03^{a}

Data are expressed as mean±standard error. Means with different superscripts in the same row are significantly different at p<0.05.

Changes in the kidney oxidative markers

Table 3 shows the mean and standard error values for the oxidative markers of the various groups. In comparison to the normal control, olive oil, DMSO, and TQ-treated groups, MDA level in the kidney tissue was noticeably higher in the rats treated with DZN. Co-treatment of the DZN group with TQ; the MDA level significantly decreased. The levels of CAT, SOD, GPx, and GSH in the kidney tissue of the rats treated with DZN were significantly lower than those of the rats in the control, olive oil, DMSO, and TQ groups. On the other hand, co-treatment of the DZN group with TQ showed significant increases in the values of CAT, SOD, GPx, and GSH.

Changes in kidney apoptotic markers

As displayed in Table 4; the rats (G5) that were treated with DZN showed that, the concentrations of BAX and IL-1β levels increased noticeably compared to normal control, olive oil, DMSO, and TQ groups after 30 days of the experiment. However, rats co-treated with both TQ and DZN (G6) had significantly lower concentrations of BAX and IL-1β levels than DZN group (G5). The rats that were treated with DZN showed that, the concentrations of BCL2 level decreased noticeably compared to normal control, olive oil, DMSO, and TQ groups after 30 days of the experiment. However, rats co-treated with both TQ and DZN (G6) had significantly higher concentration of BCL2 level than DZN group (G5).

NLRP3, Nrf2, Keap1, and NQO mRNA expression in kidney tissue

Figure 1 shows the expression of kidney NLRP3, Nrf2, Keap1, and NQO mRNA genes after 30 days of treatment in the normal control and groups treated with olive oil, DMSO, TQ, DZN, and TQ and DZN. The DZN treated rats induced a marked upregulation in kidney NLRP3, and NQO mRNA and downregulation in kidney Nrf2, and Keap1 mRNA expression. However, treatment of intoxicated rats with TQ induced a marked downregulation in NLRP3, and NQO mRNA and upregulation in kidney Nrf2, and Keap1 mRNA expression.

Changes in kidney protein markers

As displayed in Figure 2, the average relative density of kidney Nrf2, Keap1, HO-1, and NF-κB normalized to GAPDH in the TQ, DZN, and TQ-DZN-treated groups than normal control, olive oil, and DMSO treated groups after 30 days of experiment. Comparing the DZN group (G5) to the healthy control, olive oil, and DMSO treated groups, there were noticeably higher level of NF-κB as well as a substantial drop in Nrf2, Keap1, and HO-1 protein markers in kidney tissue. After 30 days of the experiment, the intoxicated group that had received TQ treatment (G6) had significantly lower level of NF-κB as well as significantly higher levels of Nrf2, Keap1, and HO-1 compared to the DZN treated group (G5).

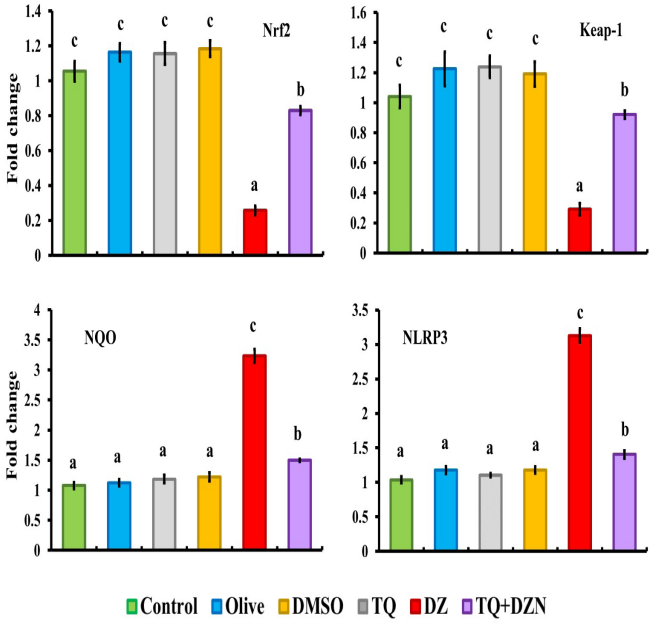

Fig. 1. Kidney Nrf2, Keap1, NQO, and NLRP3 mRNA expression. 30 days following treatments, total RNA was extracted from the kidney tissues of rats given olive oil, DMSO, thymoquinone, diazinon, thymoquinone vs diazinon, and control. Real-time PCR was used to assess expression levels, with a p-value<0.05 when compared to control values. The bars show the mean and standard error (n=6).

Histopathological assessment of kidney tissue

The DZN-treated group (G5) demonstrated swelling of renal tubular epithelial cells with vacuolization, enlarged Bowman's space, inflammatory cell infiltration, and peritubular and glomerular vascular congestion; desquamation, necrosis and interstitial edema (Figure 3d). Co-treatment of intoxicated rats with TQ showed near normal histological structure as there were decreased of Bowman's space dilatation, inflammatory cell infiltration, reduction of glomerular and peritubular vascular congestion and reduction of the renal tubular epithelium cells swelling and necrosis (Figure 3e). The kidney tissues of rats that administered olive oil, DMSO, TQ, as well as the normal control group appeared to be normal; they revealed renal corpuscles consisting of glomeruli surrounded by narrow Bowman's space and Bowman's capsule. The corpuscles were surrounded by proximal and distal convoluted tubules (Figure 3a, b, and c).

Masson's trichrome stain examination

Examination of kidney sections stained with Masson's trichrome showed that the intoxicated group (G5) displayed a significant increase in the amount of collagen fiber deposition in the interstitial tissues between the tubules and the renal corpuscles (Figure 4E). On the other hand, the intoxicated group treated with TQ (G6) showed significant decreased amounts of collagen fibers deposition in the interstitial tissues between the tubules and the

Table 4. Effect of thymoquinone (TQ) against diazinone (DZN) on apoptotic markers in the kidney homogenates of various gatherings of the experiment after 30 days of treatment, (n=6).

Groups	Control	Olive oil	DMSO	TQ	DZN	TQ+DZN
BCL2 (pg/mg protein)	144.52±3.15^{c}	160.12±2.21^{c}	153.26±2.90^{c}	158.72±1.38^{c}	59.74±3.00^{a}	133.96±4.45^{b}
BAX (ng/mg protein)	0.78±0.02^{a}	0.69±0.03^{a}	0.83±0.03^{a}	0.71±0.01^{a}	2.20±0.10^{c}	1.18±0.05^{b}
IL-1β (pg/mg protein)	54.35±1.23^{a}	57.54±1.02^{a}	56.28±0.82^{a}	51.34±1.88^{a}	126.70±2.29^{c}	70.86±2.84^{b}

Data are expressed as mean±standard error. Means with different superscripts in the same row are significantly different at p<0.05.

renal corpuscles (Figure 4F). The minimal amounts of collagen fibers among the glomerular capillaries and surrounding the renal corpuscles and tubules were detected in the normal control, olive oil, DMSO, and TQ-treated groups (Figure 4A, B, C and D).

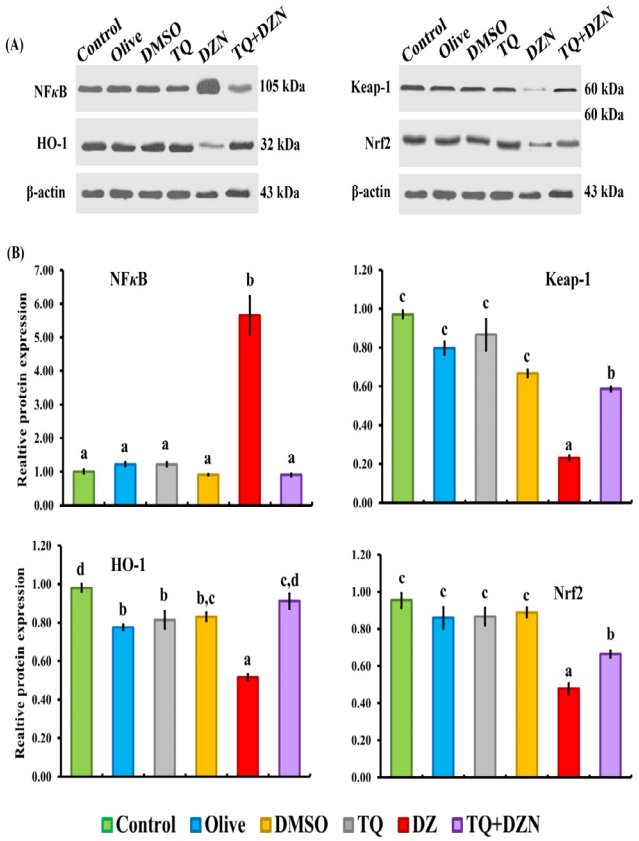

Fig. 2. Western blotting with densitometric analysis of NF-κB, HO-1, Keap1, and Nrf2 proteins in kidney tissue of rats treated with olive oil, DMSO, thymoquinone, diazinon, thymoquinone vs diazinon, and control on 30 days after treatments (n=6).

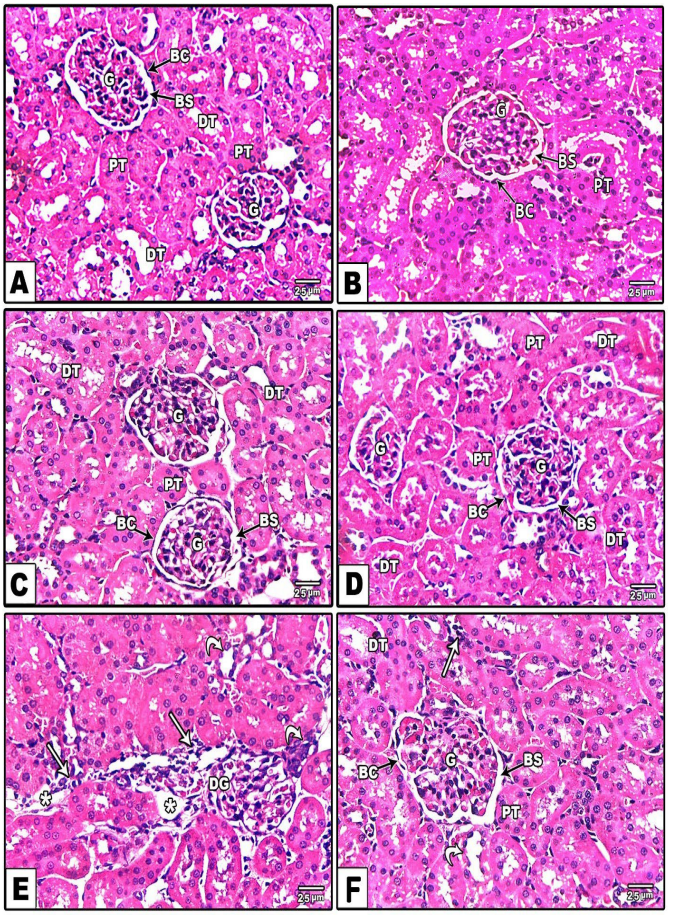

Fig. 3. Photomicrograph from kidney of experimental rats. (A), (B), and (C) Normal control rat (G1), Olive oil treated rats (G2), DMSO treated rats (G3), and rat treated with thymoquinone (G4), the kidney showed normal glomerulus (G) and Bowmen's capsule, distal tubule tubules (DT) and proximal tubules (PT). (D) Intoxicated rats (G5) induced by diazinon; showed dilatation of Bowman's space and degenerated glomeruli (DG) and inflammatory cell infiltration (arrow); glomerular and peritubular vascular congestion, swelling of renal tubular epithelium cells (curved arrow). (E) Intoxicated rat by diazinon then treated with thymoquinone, (G6), showed normal glomeruli (G) and tubules (PT andDT). (HandE,×200) (Scale bar represents 25 µm).

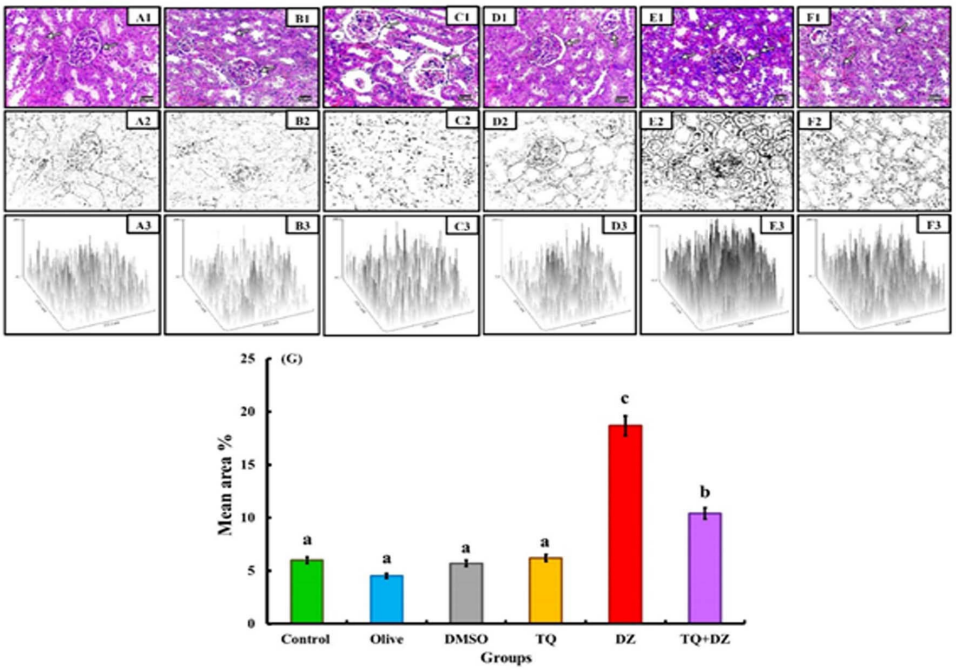

Fig. 4. Photomicrographs of kidney sections stained with Masson's trichrome; (A), (B), (C), and (D) Normal control rat (G1), Olive oil treated rats (G2), DMSO treated rats (G3) and rat treated with thymoquinone (G4), the kidney showed minimal collagen fibers among the glomerular capillaries (arrow) and surrounding the renal corpuscles and tubules (arrow). (E) Intoxicated rats (G5) induced by diazinon; the kidney showed accumulation of collagen fibers among the glomerular capillaries (arrow) and surrounding the renal corpuscles and tubules (arrow). (F) Intoxicated rat by diazinon then treated with thymoquinone (G6), showed minimal collagen fiber among the glomerular capillaries (arrow). (G) Histogram represents the mean area percentage of collagen fiber deposition in all experimental groups. (Scale bar represents 25 µm).

Immunohistochemical assessment of kidney tissue

BAX immunohistochemical staining sections of kidney tissues observed that intoxicated rats exposed to DZN (G5) showed strongly positive cytoplasmic reaction of the glomerular epithelial cells (Figure 5E). While intoxicated rats treated with TQ (G6) showed minimal positive cytoplasmic reactions of the glomerular epithelial cells (Figure 5F). BAX immunohistochemical staining sections of kidney tissues of normal control, olive oil, DMSO, and TQ-treated rats showed a minimal reaction in the glomerular epithelial cells (Figure 5A, B, C, and D).

Morphometric study

The mean area percentage of Masson's Trichrome, and BAX immuno-expression for all groups are presented in Figures 4G, and 5G respectively. The intoxicated rats treated with DZN (G5) showed a significant increase in the mean area percentage compared to normal control, olive oil, DMSO, and TQ-treated rats. While intoxicated rats treated with TQ (G6) showed significant decrease in the mean area percentage.

DISCUSSION

This research's goal was to investigate the effectiveness of TQ in maintaining renal function in Wistar rats received DZN to induce nephrotoxicity. Due to its numerous health advantages and lack of negative side effects as compared to synthetic medications, over the past few decades, there has been an increase in the use of herbal remedies and other substances derived from plants as complementary treatments for a variety of pathological conditions (Mahmoodi and Mohammadizadeh, 2020). In this study, DZN at a dose of 15 mg/kg body weight had no clinically significant adverse effects, and the rats showed no signs of stress.

This study revealed that serum urea and creatinine levels significantly increased in G5 that was received DZN. The elevated level of serum urea and creatinine may be due to the nephrotoxicity of DZN. When intoxicated rats were given TQ (G6), the levels of blood urea and creatinine significantly dropped. The TQ's nephroprotective activity, which also has anti-inflammatory and antioxidant effects, may be to blame for this outcome. These results agreed with those of earlier study (Zhang *et al*., 2020).

The results of the current study showed that after receiving DZN for 30 days, the intoxicated group's MDA value dramatically increased while their CAT, SOD, GPx, and GSH values significantly reduced, indicating oxidative stress. The increased levels of MDA and decreased levels of CAT, SOD, GPx, and GSH may have been caused by DZN's ability to cause tissue damage by producing nephrotoxicity, which raises the levels of lipid peroxidation by-products and lowers the levels of antioxidants (Nili-Ahmadabadi *et al*., 2018). Among the detrimental effects of lipid peroxidation include increased membrane rigidity, the release of the amino acid tyrosine into the extracellular medium, osmotic fragility, decreased cellular and subcellular components, increased ROS generation, and lipid fluidity (Shah and Iqbal, 2010). The MDA induction agrees with Jafari *et al*. (2012). On the other hand, TQ treatment of intoxicated rats resulted in a much lower level of MDA and a significantly higher level of CAT, SOD, GPx, and GSH. TQ possesses antioxidant capacity, and these results support the findings of Danaei *et al*. (2019) who noted the antioxidant effects of TQ in the heart.

The present study revealed that BAX, and IL-1β levels significantly increased while BCL-2 was significantly decreased in G5 that was received DZN. TQ treatment of intoxicated rats resulted in a significant increase in BCL-2 levels while a considerable decrease in BAX and IL-1β levels. Oxidative stress is a known apoptotic promoter as BCL-2 protein family regulates mitochondrial apoptosis (Malik *et al*., 2016). The pro-apoptotic BAX, IL-1β, and the anti-apoptotic BCL-2 are two crucial players in controlling the process of mitochondrial apoptosis (Adams and Cory, 2018). Additionally, Caspase-3 is one of the crucial signaling pathway mediators for apoptosis, and its activation ultimately results in apoptosis (Kosenko *et al*., 2014). The release of Cyt-c and the activation of downstream caspase-3 proteases, which regulate cell survival or death, can be regulated by their overexpression (Olivetti *et al*., 1997).

The kidneys of TQ-treated rats showed improved histopathological images, when compared to the kidneys of rats treated with DZN, which revealed dilated Bowman's space, inflammatory

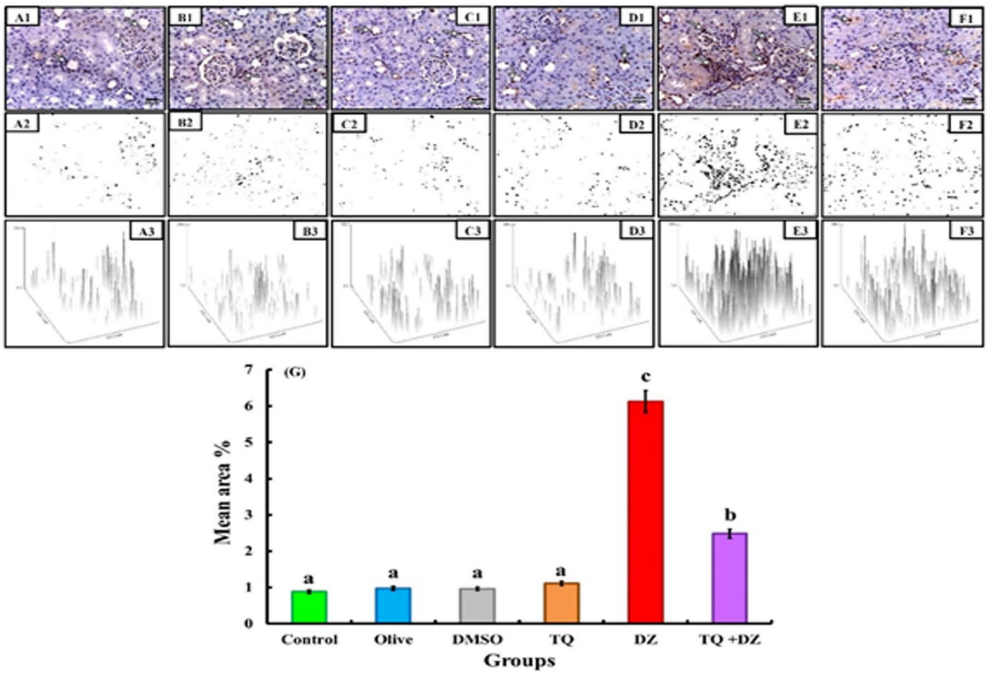

Fig. 5. BAX immunohistochemical staining sections of kidney of experimental rats. (A), (B), (C), and (D) Normal control rats (G1), Olive oil treated rats (G2), DMSO treated rats (G3), and rats treated with thymoquinone (G4), showed minimal reaction in the glomerular epithelial cells. (E) Intoxicated rats (G5) induced by diazinon; showed strong positive cytoplasmic reaction in glomerular epithelial cells (arrow). (F) Intoxicated rat by diazinon then treated with thymoquinone (G6), showed minimal positive cytoplasmic reaction in the glomerular epithelial cells (arrow). (G) Histogram representing the mean area percentage of BAX immunoreaction in all experimental groups. (Anti-BAX, ×400) (Scale bar represents 25 μm).

cell infiltration, congested glomerular and peritubular vascular structures, and swollen renal tubular epithelium cells with vacuolization, desquamation, necrosis and interstitial edema. These findings coincided with (Al-Attar, 2015). In addition, examination of kidney sections of DZN-treated rats stained with Masson's trichrome showed that a significant increase in the amount of collagen fiber deposition in the interstitial tissues between the tubules and the renal corpuscles. These findings coincided with Tsai *et al.* (2020). The BAX immunohistochemical staining sections of DZN-treated rats showed strongly positive cytoplasmic reaction of the glomerular epithelial cells. These results were in agreement with those of earlier study (Mahboub and Arisha, 2015). While intoxicated rats treated with TQ resulted in near normal histological structure as there were reduction in Bowman's space dilatation, inflammatory cell infiltration, and reduction of glomerular and peritubular vascular congestion as well as reduction of the renal tubular epithelium cells swelling and necrosis. These findings coincided with Hannan *et al.* (2021). In addition, examination of kidney sections of intoxicated rats treated with TQ stained with Masson's trichrome showed a significant decreased amounts of collagen fibers deposition in the interstitial tissues between the tubules and the renal corpuscles. These findings coincided with Bargi *et al.* (2017). The BAX immunohistochemical staining sections of intoxicated rats treated with TQ showed minimal positive cytoplasmic reactions of the glomerular epithelial cells. These results concurred with those reported by Hashem *et al.* (2021).

The present study revealed a marked increase in the NF-κB with marked decrease in Nrf2, Keap1, and HO-1 protein markers in kidney tissue that confirmed by significant upregulation in kidney NLRP3, and NQO mRNA with marked downregulation in Nrf2, and Keap1 mRNA observed in the intoxicated group at 30 days of receiving DZN, which indicates pyroptosis-mediated cell death.

NF-κB, as the main transcriptional regulator of inflammation-related genes, plays a significant role in inflammation and important in the pathophysiology of renal diseases (Leslie *et al*., 2013), through transcription of pro-inflammatory cytokines and chemokines (Knauf *et al*., 2019). However, many studies have shown that there is an interaction between NF-κB and Nrf2 pathway in inflammation; as Keap1 inhibits the activity of NF-κB through ubiquitin degradation of IκB kinase-β (Lee *et al*., 2009). The inflammatory process can induce inflammatory mediators, which react with Keap1 to activate Nrf2, to initiate gene transcription while inhibiting NF-κB activity (Klotz *et al*., 2015). NF-κB can bind to CREB-binding protein (CBP), a competitive Nrf2 transcriptional coactivator (Li *et al*., 2020). The functional binding sites of NF-κB in the promoter of rat and mouse HO-1 gene have been identified. This HO-κB binding can act on NF-κB and over expression of NF-κB can activate HO-1, which indicates the interaction between NF-κB and HO-1 in Nrf2/ARE (El-Shaer *et al*., 2021). ROS generation leads to the activation of NLRP3 infammasome, thereby inducing kidney injury (Xie *et al*., 2022). NLRP3 is an inflammasome complex whose dysregulated activation is associated with kidney damage and sepsis (Yang *et al*., 2021). NLRP3 was reported to regulate the maturation of IL-18 and IL-1β, via recruitment and activation of caspase-1, and thereby induce inflammatory cell death (pyroptosis) (Ruiz-Baca *et al*., 2021). On the other side, intoxicated group treated with TQ showed significant decreases in the level of NF-κB with marked increase in Nrf2, Keap1, and HO-1 protein markers in kidney tissue that confirmed by significant downregulation in kidney NLRP3, and NQO mRNA with marked upregulation in Nrf2, and Keap1 mRNA at 30 days of experiment. These findings attributed to anti-inflammatory effects of TQ via inhibiting NLRP3 inflammasome. These findings agree with (Liu *et al*., 2019); who explained the potential protective mechanisms of TQ in attenuated cardiac injury via reducing the expression of NLRP3. Also, the present findings agree with Dai *et al.* (2019); who explained the potential protective mechanisms of melatonin in attenuated sepsis-induced renal injury. The inhibition of NF-κB was shown to reduce kidney injury (Song *et al*., 2019). TQ treatment decreased the expression of NF-κB and inhibited the inflammatory cascade. The upregulation of Nrf2 level may be due to the regulation of gene expression by NF-κB (Liu *et al*., 2016). The Nrf2 can bind to the ARE sequence upstream of BCL-2 and cause its upregulation (Gupta *et al*., 2019). One possible explanation is that TQ protects renal cells from DZN-induced apoptosis by activating the Nrf2 pathway. Nrf2 was accumulated and transferred to the nuclear region of ARE. ARE regulates phase II detoxification and induces antioxidant enzyme expressions, including NQO and HO-1 (Mathur *et al*., 2016). HO-1 plays an anti-apoptotic effect (Fang *et al*., 2004). TQ activates Nrf2 pathway in a Keap1-dependent manner (Jin *et al*., 2020).

CONCLUSION

Kidney injury as one of the complications that result from intoxication with DZN; is mediated by pyroptosis which is induced by triggering NF-κB-HO-1-Keap1-Nrf2 pathway. DZN-induced kidney dysfunction is effectively ameliorated with the use of TQ via inactivating NF-κB-mediated pyroptosis, which may be a new strategy to mitigate renal complications. This study has not only elaborated on the underlying pathology of DZN-induced kidney injury, but also provided a background for possible therapeutics that may prove beneficial.

CONFLICT OF INTEREST

The authors declare that they have no competing interests.

REFERENCES

Adams, J.M., Cory, S., 2018. The BCL-2 arbiters of apoptosis and their growing role as cancer targets. Cell Death and Differentiation 25, 27-36.

Al-Attar, A.M., 2015. Effect of grapeseed oil on diazinon-induced physiological and histopathological alterations in rats. Saudi journal of biological sciences 22, 284-292.

Bargi, R., Asgharzadeh, F., Beheshti, F., Hosseini, M., Farzadnia, M., Khazaei, M., 2017. Thymoquinone protects the rat kidneys against renal fibrosis. Research in pharmaceutical sciences 12, 479.

Boussabbeh, M., Ben Salem, I., Hamdi, M., Ben Fradj, S., Abid-Essefi, S., Bacha, H., 2016. Diazinon, an organophosphate pesticide, induces oxidative stress and genotoxicity in cells deriving from large intestine. Environmental Science and Pollution Research 23, 2882-2889.

Bradford, M.M., 1976. A rapid and sensitive method for the quantitation of microgram quantities of protein utilizing the principle of protein-dye binding. Analytical biochemistry 72, 248-254.

Dai, W., Huang, H., Si, L., Hu, S., Zhou, L., Xu, L., Deng, Y., 2019. Melatonin prevents sepsis-induced renal injury via the PINK1/Parkin1 signaling pathway. International Journal of Molecular Medicine 44, 1197-1204.

Danaei, G.H., Karami, M., 2017. Protective effect of thymoquinone against diazinon-induced hematotoxicity, genotoxicity and immunotoxicity in rats. Environmental Toxicology and Pharmacology 55, 217-222.

Danaei, G.H., Memar, B., Ataee, R., Karami, M., 2019. Protective effect of thymoquinone, the main component of *Nigella sativa*, against diazinon cardio-toxicity in rats. Drug and Chemical Toxicology 42, 585-591.

Fang, J., Akaike, T., Maeda, H., 2004. Antiapoptotic role of heme oxygenase (HO) and the potential of HO as a target in anticancer treatment. Apoptosis 9, 27-35.

Guignet, M., Dhakal, K., Flannery, B.M., Hobson, B.A., Zolkowska, D., Dhir, A., Bruun, D.A., Li, S., Wahab, A., Harvey, D.J., 2020. Persistent behavior deficits, neuroinflammation, and oxidative stress in a rat model of acute organophosphate intoxication. Neurobiology of disease 133, 104431.

Gupta, P., Choudhury, S., Ghosh, S., Mukherjee, S., Chowdhury, O., Sain, A., Chattopadhyay, S., 2019. Dietary pomegranate supplement alleviates murine pancreatitis by modulating Nrf2-p21 interaction and controlling apoptosis to survival switch. The Journal of Nutritional Biochemistry 66, 17-28.

Hannan, M.A., Zahan, M.S., Sarker, P.P., Moni, A., Ha, H., Uddin, M.J., 2021. Protective effects of black cumin (*Nigella sativa*) and its bioactive constituent, thymoquinone against kidney injury: An aspect on

pharmacological insights. International Journal of Molecular Sciences 22, 9078.

Hashem, K.S., Abdelazem, A.Z., Mohammed, M.A., Nagi, A.M., Aboulhoda, B.E., Mohammed, E.T., Abdel-Daim, M.M., 2021. Thymoquinone alleviates mitochondrial viability and apoptosis in diclofenac-induced acute kidney injury (AKI) via regulating Mfn2 and miR-34a mRNA expressions. Environmental Science and Pollution Research 28, 10100-10113.

Hegazy, A.M., Hafez, A.S., Eid, R.M., 2020. Protective and antioxidant effects of copper-nicotinate complex against glycerol-induced nephrotoxicity in rats. Drug and Chemical Toxicology 43, 234–239.

Jafari, M., Salehi, M., Ahmadi, S., Asgari, A., Abasnezhad, M., Hajigholamali, M., 2012. The role of oxidative stress in diazinon-induced tissues toxicity in Wistar and Norway rats. Toxicology Mechanisms and Methods 22, 638-647.

Jakhmola Mani, R., Sehgal, N., Dogra, N., Saxena, S., Pande Katare, D., 2022. Deciphering underlying mechanism of Sars-CoV-2 infection in humans and revealing the therapeutic potential of bioactive constituents from *Nigella sativa* to combat COVID19: in-silico study. Journal of Biomolecular Structure and Dynamics 40, 2417-2429.

Jiang, F., Peng, Y., Sun, Q., 2022. Pesticides exposure induced obesity and its associated diseases: recent progress and challenges. Journal of Future Foods 2, 119-124.

Jin, W., Zhang, Y., Xue, Y., Han, X., Zhang, X., Ma, Z., Sun, S., Chu, X., Cheng, J., Guan, S., 2020. Crocin attenuates isoprenaline-induced myocardial fibrosis by targeting TLR4/NF-κB signaling: connecting oxidative stress, inflammation, and apoptosis. Naunyn-Schmiedeberg's Archives of Pharmacology 393, 13-23.

Kizi, K.S.A., Kizi, A.B.J., 2022. THERAPEUTIC POTENTIAL OF *Nigella sativa*: A MIRACLE HERB. European International Journal of Multidisciplinary Research and Management Studies 2, 259-262.

Klotz, L.-O., Sánchez-Ramos, C., Prieto-Arroyo, I., Urbánek, P., Steinbrenner, H., Monsalve, M., 2015. Redox regulation of FoxO transcription factors. Redox Biology 6, 51-72.

Knauf, F., Brewer, J.R., Flavell, R.A., 2019. Immunity, microbiota and kidney disease. Nature Reviews Nephrology 15, 263-274.

Kosenko, E.A., N Solomadin, I., A Tikhonova, L., Prakash Reddy, V., Aliev, G., G Kaminsky, Y., 2014. Pathogenesis of Alzheimer disease: role of oxidative stress, amyloid-β peptides, systemic ammonia and erythrocyte energy metabolism. CNS and Neurological Disorders-Drug Targets (Formerly Current Drug Targets-CNS and Neurological Disorders) 13, 112-119.

Lee, D.-F., Kuo, H.-P., Liu, M., Chou, C.-K., Xia, W., Du, Y., Shen, J., Chen, C.-T., Huo, L., Hsu, M.-C., 2009. KEAP1 E3 ligase-mediated downregulation of NF-κB signaling by targeting IKKβ. Molecular cell 36, 131-140.

Leslie, K.L., Song, G.J., Barrick, S., Wehbi, V.L., Vilardaga, J.-P., Bauer, P.M., Bisello, A., 2013. Ezrin-radixin-moesin-binding phosphoprotein 50 (EBP50) and nuclear factor-κB (NF-κB): a feed-forward loop for systemic and vascular inflammation. Journal of Biological Chemistry 288, 36426-36436.

Li, S., Eguchi, N., Lau, H., Ichii, H., 2020. The role of the Nrf2 signaling in obesity and insulin resistance. International Journal of Molecular Sciences 21, 6973.

Liu, H., Sun, Y., Zhang, Y., Yang, G., Guo, L., Zhao, Y., Pei, Z., 2019. Role of thymoquinone in cardiac damage caused by sepsis from BALB/c mice. Inflammation 42, 516-525.

Liu, X., Zhang, X., Ma, K., Zhang, R., Hou, P., Sun, B., Yuan, S., Wang, Z., Liu, Z., 2016. Matrine alleviates early brain injury after experimental subarachnoid hemorrhage in rats: possible involvement of PI3K/Akt-mediated NF-Î°B inhibition and Keap1/Nrf2-dependent HO-1 inductionn. Cellular and Molecular Biology 62, 38-44.

Livak, K.J., Schmittgen, T.D., 2001. Analysis of relative gene expression data using real-time quantitative PCR and the $2^{-\Delta\Delta CT}$ method. methods 25, 402-408.

Mahboub, F.A., Arisha, S.M., 2015. Hepatoprotective effect of Ocimum basilicum extract against the toxicity of diazinon in albino rats: Histopathological and immunohistochemical evaluation. World Journal of Pharmaceutical Sciences 2015, 790-799.

Mahmoodi, M.R., Mohammadizadeh, M., 2020. Therapeutic potentials of *Nigella sativa* preparations and its constituents in the management of diabetes and its complications in experimental animals and patients with diabetes mellitus: A systematic review. Complementary Therapies in Medicine 50, 102391.

Malik, S., Suchal, K., Bhatia, J., Khan, S.I., Vasisth, S., Tomar, A., Goyal, S., Kumar, R., Arya, D.S., Ojha, S.K., 2016. Therapeutic potential and molecular mechanisms of Emblica officinalis Gaertn in countering Nephrotoxicity in rats induced by the chemotherapeutic agent Cisplatin. Frontiers in Pharmacology 7, 350.

Mathur, A., Rizvi, F., Kakkar, P., 2016. PHLPP2 down regulation influences nuclear Nrf2 stability via Akt-1/Gsk3β/Fyn kinase axis in acetaminophen induced oxidative renal toxicity: Protection accorded by morin. Food and Chemical Toxicology 89, 19-31.

Nili-Ahmadabadi, A., Alibolandi, P., Ranjbar, A., Mousavi, L., Nili-Ahmadabadi, H., Larki-Harchegani, A., Ahmadimoghaddam, D., Omidifar, N., 2018. Thymoquinone attenuates hepatotoxicity and oxidative damage caused by diazinon: an in vivo study. Research in Pharmaceutical Sciences 13, 500.

Olivetti, G., Abbi, R., Quaini, F., Kajstura, J., Cheng, W., Nitahara, J.A., Quaini, E., Di Loreto, C., Beltrami, C.A., Krajewski, S., 1997. Apoptosis in the failing human heart. New England Journal of Medicine 336, 1131-1141.

Prairna, B., Khan, J., Ali, A., 2022. Therapeutic potential of *Nigella sativa* in the prevention of aggregation and glycation of proteins. in: Black Seeds (*Nigella sativa*), Elsevier, pp. 313-336.

Rashedinia, M., Hosseinzadeh, H., Imenshahidi, M., Lari, P., Razavi, B.M., Abnous, K., 2016. Effect of exposure to diazinon on adult rat's brain. Toxicology and Industrial Health 32, 714-720.

Ruiz-Baca, E., Pérez-Torres, A., Romo-Lozano, Y., Cervantes-García, D., Alba-Fierro, C.A., Ventura-Juárez, J., Torriello, C., 2021. The role of macrophages in the host's defense against Sporothrix schenckii. Pathogens 10, 905.

Salem, M.A., El-Shiekh, R.A., Aborehab, N.M., Al-Karmalawy, A.A., Ezzat, S.M., Alseekh, S., Fernie, A.R., 2023. Metabolomics driven analysis of *Nigella sativa* seeds identifies the impact of roasting on the chemical composition and immunomodulatory activity. Food Chemistry 398, 133906.

Shah, M.D., Iqbal, M., 2010. Diazinon-induced oxidative stress and renal dysfunction in rats. Food and Chemical Toxicology 48, 3345-3353.

Skeggs, L.T., 1957. An automatic method for colorimetric analysis. American journal of clinical pathology 28, 311-322.

Song, N., Thaiss, F., Guo, L., 2019. NFκB and kidney injury. Frontiers in Immunology 10, 815.

Suvarna, K.S., Layton, C., Bancroft, J., 2013. Immunohistochemical techniques. Bancroft's Theory and Practice of Histological Techniques. 7th ed., Churchill Livingstone, Philadelphia 381-426.

Suvarna, K.S., Layton, C., Bancroft, J.D., 2018. Bancroft's theory and practice of histological techniques E-Book. Elsevier Health Sciences.

Tsai, B.C.-K., Kuo, W.-W., Day, C.H., Hsieh, D.J.-Y., Kuo, C.-H., Daddam, J., Chen, R.-J., Padma, V.V., Wang, G., Huang, C.-Y., 2020. The soybean bioactive peptide VHVV alleviates hypertension-induced renal damage in hypertensive rats via the SIRT1-PGC1α/Nrf2 pathway. Journal of Functional Foods 75, 104255.

Wang, J., Teng, Y., Zhai, Y., Yue, W., Pan, Z., 2022. Spatiotemporal distribution and risk assessment of organophosphorus pesticides in surface water and groundwater on the North China Plain, China. Environmental Research 204, 112310.

Weissman, M., Pileggi, V., Henry, R., Cannon, D., Winkelman, J., 1974. Clinical chemistry: principles and techniques, Harper and Row Publishers, Hagerstown, MD.

Xie, H., Peng, J., Zhang, X., Deng, L., Ding, Y., Zuo, X., Wang, F., Wu, Y., Zhang, J., Zhu, Q., 2022. Effects of mitochondrial reactive oxygen species-induced NLRP3 inflammasome activation on trichloroethylene-mediated kidney immune injury. Ecotoxicology and Environmental Safety 244, 114067.

Yang, M., Fang, J.-t., Zhang, N.-s., Qin, L.-j., Zhuang, Y.-y., Wang, W.-w., Zhu, H.-p., Zhang, Y.-j., Xia, P., Zhang, Y., 2021. Caspase-1-inhibitor AC-YVAD-CMK inhibits pyroptosis and ameliorates acute kidney injury in a model of sepsis. BioMed Research International 2021, 1-9.

Yu, Z.-W., Zhang, J., Li, X., Wang, Y., Fu, Y.-H., Gao, X.-Y., 2020. A new research hot spot: The role of NLRP3 inflammasome activation, a key step in pyroptosis, in diabetes and diabetic complications. Life sciences 240, 117138.

Zhang, R., Zhu, Y., Li, Y., Liu, W., Yin, L., Yin, S., Ji, C., Hu, Y., Wang, Q., Zhou, X., 2020. Human umbilical cord mesenchymal stem cell exosomes alleviate sepsis-associated acute kidney injury via regulating microRNA-146b expression. Biotechnology letters 42, 669-679.